

Iterative 3D Projection Reconstruction of ^{23}Na Data with a ^1H -MRI Constraint

Christine Gnahn¹, Michael Bock^{1,2}, Wolfhard Semmler¹, and Armin M. Nagel¹

¹Dept. of Medical Physics in Radiology, German Cancer Research Center (DKFZ), Heidelberg, Germany, ²Radiology - Medical Physics, University Hospital Freiburg, Freiburg, Germany

Introduction

Non-proton MRI, such as the imaging of ^{23}Na , provides access to functional tissue information. The cellular sodium concentration is altered in many diseases like myocardial infarction and cancer [1]. However, non-proton MRI generally suffers from low signal-to-noise ratios (SNR) and long measurement times. On the other hand, high resolution proton images with excellent SNR can be acquired within a few minutes. Thus, it would be desirable to use the ^1H information to improve the quality of non-proton images. Different attempts have been made to improve low SNR images by anatomically constrained reconstructions [2,3,4]. In this work, an iterative reconstruction using a simple ^1H image derived constraint in combination with a total variation (TV) penalty is used to improve the SNR and to reduce undersampling artifacts and Gibbs ringing in ^{23}Na images.

Methods

a) *MR-measurements*: ^{23}Na - and ^1H -MRI were performed on a clinical 3T MR-system (Magnetom TIM Trio 3T, Siemens Healthcare, Erlangen, Germany) using a double resonant ($^{23}\text{Na}/^1\text{H}$), single channel quadrature birdcage coil (Rapid Biomedical GmbH, Rimpar, Germany). Co-registered ^{23}Na - and ^1H -images of a resolution phantom and the brain of a healthy volunteer were acquired. For SNR evaluation, an additional noise measurement without RF-pulses was obtained. The following parameters were used for ^{23}Na -MRI with a density-adapted 3D projection reconstruction sequence (DA-3DPR) [5]: TE/TR = 0.3ms/80ms, $\alpha = 85^\circ$, readout time = 40ms, nominal resolution $\Delta x^3 = (4\text{mm})^3$. In total, 10000/2000/1000 projections were acquired, corresponding to undersampling factors (USF) of 1/5/10. ^1H -images were obtained with a 3D-FLASH sequence.

b) *Prior knowledge constrained image reconstruction*: The images were reconstructed iteratively by minimizing an objective function [6] using a Conjugate Gradient algorithm [7]. In addition to the data consistency term, the objective function contained two regularization terms: A TV-constraint and a new constraint, using ^1H image information to penalize nonzero pixel intensities outside the imaged object (which must be either noise or artifact) with a squared L2-norm. The corresponding regularization term (BM) was $R_{BM}(x) = \tau_{BM} \|BM \cdot x\|_2^2$, with the constant weighing factor τ_{BM} (best results were achieved with $\tau_{BM} = 1$), the ^{23}Na image x and the ^1H image derived binary mask BM (Fig. 1c). The algorithm was implemented in C++ using the FFTW3-library. For comparison, data were also reconstructed using conventional gridding and iterative reconstruction with TV-regularization alone.

c) *Reconstruction evaluation*: For quantitative SNR evaluation, bootstrapped statistics were used to calculate SNR maps with 100 replica [8] for all reconstructions. To verify that different sodium concentrations were reconstructed correctly, the phantom contained six tubes filled with NaCl-solutions at concentrations between 0.2 and 1.2% (Fig. 1a). For each tube, the mean pixel intensity within a region of interest was calculated for one representable slice. The coefficient of determination for the linear fit through these values (R^2) was taken as a measure for the concentration reproducibility.

Results

^{23}Na images reconstructed from data with different USFs are shown in Fig. 2. SNR and R^2 -values are listed in table 1. All reconstruction algorithms could reproduce the sodium concentrations ($R^2 > 0.95$). For USF=10, the R^2 value is slightly higher with the iterative TV&BM-reconstruction. Furthermore, the streaking artifacts visible in the gridding reconstruction (Fig. 2b and 2c) are considerably reduced by the iterative reconstructions (Fig. 2e-f and 2h-i). SNR is significantly increased by both iterative reconstruction techniques (TV&BM: 50% for USF = 1, 140% for USF = 5 / 10; TV: 70% for USF = 1 up to 600% for USF = 10). Particularly for the largest USF of 10, the advantage of the TV&BM-regularization over a mere TV-constraint becomes evident: The smallest structures are still visible in Fig. 2f, but cannot be distinguished in Fig. 2i. At a lower USF of 5, the iterative TV&BM-reconstruction (Fig. 2e) shows comparable SNR, contrast and concentration values as the gridding reconstruction of the fully sampled data (Fig. 2a). The quality improvement with TV&BM algorithm could also be seen in the *in vivo* images of a healthy volunteer, where an average SNR increase of 33% for an USF of 2 is found (Fig. 3).

Discussion

The proposed constraint uses only the most elementary anatomical information, i.e. the object boundary; nevertheless, it allows reconstructing more image details than an iterative reconstruction with a TV-constraint. This is in contrast to the algorithm presented in reference [3], where features that were not known *a priori* are reconstructed with lower resolution. Additionally, the TV&BM-regularization does not alter the image contrast, which is of utmost importance for concentration quantification. In future refinements of the algorithm it will be evaluated whether a higher spatial resolution can be achieved using more advanced constraints (e.g. the inclusion of anatomical details).

References

1. Boada et al., Curr Top Dev Biol (2005) 70, 77-101.
2. Constantinides et al., Magn Reson Imaging (2000) 18, p. 461-471.
3. Haldar et al., Magn Reson Med (2008) 59, p. 810-818.
4. Atkinson et al., Proc Intl Soc Mag Reson Med 16 (2008), p. 335.
5. Nagel et al., Magn Reson Med (2009) 62, p. 1565-1573.
6. Block et al., Magn Reson Med (2007) 57, p. 1086-1098.
7. Zhang et al., IMA JNA (2006) 26, p. 629-640.
8. Riffe et al., Proc Intl Soc Mag Reson Med (2007), p. 1879.

Acknowledgement

The authors would like to thank Dr. Martin Uecker for his kind and helpful explanations.

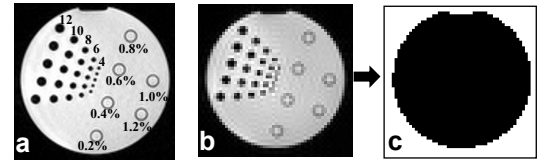


Fig. 1: a) ^1H -image of a resolution phantom with structure diameters in mm. The 6 tubes on the right contain NaCl-solutions at different concentrations. The residual volume of the phantom is filled with 0.6% NaCl-solution. b) ^1H image ($\Delta x^3 = (4\text{mm})^3$) of the resolution phantom and c) derived binary mask (BM) used in the reconstruction.

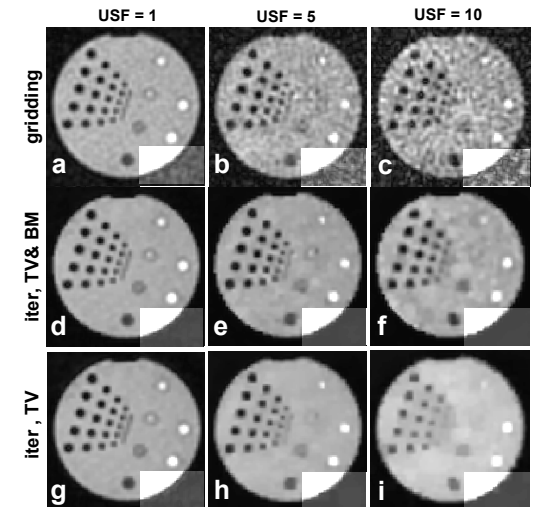


Fig. 2: ^{23}Na -images ($\Delta x^3 = (4\text{mm})^3$) with USF of 2 to 10 for different reconstruction algorithms. In the lower right corner, the images are scaled differently to enhance image noise and artifacts.

	SNR			R ²		
	USF 1	USF 5	USF 10	USF 1	USF 5	USF 10
gridding	30	14	10	0.996	0.989	0.967
iterative, TV&BM	46	33	24	0.998	0.978	0.980
iterative, TV	51	68	70	0.998	0.975	0.950

Table 1: Mean SNR values and R^2 -values for the linear fit to measured sodium concentrations in the ^{23}Na reconstructions shown in Fig. 2.

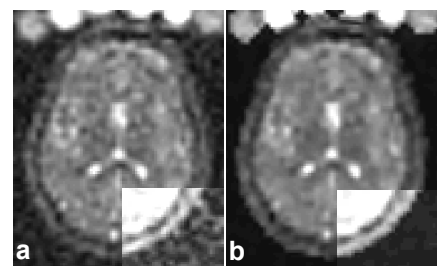


Fig. 3: ^{23}Na brain images of a healthy volunteer ($\Delta x^3 = (4\text{mm})^3$). a) Gridding reconstruction. b) Iterative reconstruction with TV&BM-regularization.